FULL PAPER

Dalton
www.rsc.org/dalton

Supramolecular variations on a molecular theme: the structural diversity of phosphazenes $(RNH)_6P_3N_3$ in the solid state

Jamie F. Bickley, Richard Bonar-Law, Gavin T. Lawson, Philip I. Richards, Frederic Rivals, Alexander Steiner * and Stefano Zacchini

Department of Chemistry, University of Liverpool, Crown Street, Liverpool, UK L69 7ZD. E-mail: a.steiner@liv.ac.uk

Received 11th December 2002, Accepted 13th February 2003
First published as an Advance Article on the web 26th February 2003

Herein, we introduce an extremely 'soft' tecton, which interacts *via* 'soft' synthons displaying an unprecedented variety of supramolecular architectures in the solid state. Hexakis(organoamino) cyclotriphosphazene derivatives, $(RNH)_6P_3N_3$, contain a polar core comprising an equatorial belt of three ring nitrogen atoms and six NH functions which is sandwiched between hemispheres of lipophilic substituents R. A range of derivatives equipped with hydrocarbon side chains were synthesised and structurally characterised including R = *tert*-butyl (**1**), cyclohexyl (**2**), *iso*-propyl (**3**), benzyl (**4**), 2-phenylethyl (**5**), *iso*-butyl (**6**), phenyl (**7**), *p*-tolyl (**8**), *n*-propyl (**9**), allyl (**10**), propargyl (**11**) and methyl (**12**). The study shows that subtle modifications of the lipophilic periphery lead to considerable changes in the solid-state aggregation pattern. With the exception of **1** all solid-state structures show intermolecular NH ··· N bonding with motifs containing one, two, three and four H-bridges. Supramolecular architectures include monomer (**1**), dimer (**2**), cyclic hexamer (**3**), zigzag chain (**4**, **6**), linear chain (**5**·thf, **7**, **8**), double chain (**9**), graphite-type sheet (**10**), rectangular grid (**11**) and hexagonal close-packed sheet (**12**). The structural variety is due to easy rotation around exocyclic P–N bonds, which allows variable directionalities of all six N–H bonds. M.O. calculations on the gas phase dimer of $(H_2N)_6P_3N_3$ mirror the H-bridging motifs observed in crystal structures of $(RNH)_6P_3N_3$ derivatives.

Introduction

The arrangement of molecules in the solid state is governed by a delicate interplay of non-covalent forces and packing factors. Intermolecular interactions vary widely in strength, ranging from relatively strong and directional hydrogen bonding between electronegative atoms down to weak non-directional dispersion forces between hydrocarbon chains.[1] The steadily growing field of crystal engineering exploits the hierarchy of non-covalent interactions with the aim of producing single crystal materials.[2] Hence, there is an ongoing search for new molecular building blocks (*tectons*), which can interact *via* spatial arrangements of attractive 'sticky' sites (*supramolecular synthons*), inducing the assembly of supramolecular aggregates.[3] In general, stereo-rigid ('hard') tectons which interact *via* robust synthons crystallise with unambiguous supramolecular geometries, whereas more flexible ('soft') tectons and less robust synthons often facilitate the formation of supramolecular isomers.

Classic examples of 'hard' tectons are crystal structures of benzene polycarboxylic acids, featuring a stereo-rigid benzene core bearing the robust carboxylic acid dimer synthon. The number and relative positions of $-CO_2H$ groups around the benzene ring determine the structure and dimensionality of the resulting network. For example, benzene-1,4-dicarboxylic acid forms linear 1-D chains,[4] benzene-1,3,5-tricarboxylic acid hexagonal 2-D sheets[5] and adamantane-1,3,5,7-tetracarboxylic acid diamondoid 3-D networks.[6] Benzene-1,3-dicarboxylic acid, on the other hand, displays an ambivalent supramolecular behaviour. The 120° angle between two carboxylic acids facilitates both *trans* (polymeric zigzag chain) and *cis* arrangements (cyclic hexamer). Some control over the supramolecular structure can be obtained by introducing lipophilic alkoxy substituents with alkyl chains of different lengths in the 5-position of the benzene ring.[7] Other examples featuring supramolecularly ambivalent tectons are co-crystals of melamine and barbituric acid derivatives, which interact *via* triads of hydrogen bonds. Varying the sizes of lipophilic substituents on both components induces the formation of either linear tapes, crinkled tapes or cyclic "rosette" structures.[8] Amphiphilic tectons with spatially separated polar and non-polar regions form increasingly diverse supramolecular arrangements as the tecton becomes more flexible and the synthon weaker. Consequently, with increasing 'softness' of both tectons and synthons, the supramolecular structure is largely controlled by the size and shape of the lipophilic moiety. This is nicely demonstrated by the structural diversity of silanetriols, $RSi(OH)_3$. This 'soft' tecton contains a tetrahedral silicon core with free rotation around Si–R and Si–OH bonds. All three hydroxy groups can act as both hydrogen bond donors and acceptors, forming extensive networks of OH ··· O bonds. The bulkiness of the lipophilic R-group determines their aggregation pattern, which include hexameric cages,[9] tubular columns,[10] layers[11] and double layers.[12] However, silanetriols are of low kinetic stability and readily undergo condensation reactions to form polysiloxanes.

Herein, we introduce an extremely 'soft' tecton, which interacts *via* 'soft' synthons displaying an unprecedented variety of supramolecular architectures in the solid state. Hexakis(organoamino) cyclotriphosphazene derivatives, $(RNH)_6P_3N_3$, contain a polar core comprising an equatorial belt of three ring nitrogen atoms and six NH functions which are sandwiched between hemispheres of lipophilic substituents R (Fig. 1). Such phosphazenes show amphiprotic behaviour: the N(ring) sites are basic with pK_as similar to primary amines[13] and the NH groups can be deprotonated by strong organometallic bases.[14] This array of three basic N and six acidic NH sites suggests various possibilities for intermolecular NH ··· N hydrogen bonding. Unhindered rotation around the six P–NH bonds allow the N–H bonds to point in various directions leading to smooth synthon-transformations. We have equipped $(RNH)_6P_3N_3$ with hydrocarbon substituents R of various size and shape in order to investigate their aggregation behaviour in the solid-state. Substituents include R = *tert*-butyl (**1**), cyclohexyl (**2**), *iso*-propyl (**3**), benzyl (**4**), 2-phenylethyl (**5**), *iso*-butyl (**6**), phenyl (**7**), *p*-tolyl (**8**), *n*-propyl (**9**), allyl (**10**), propargyl (**11**) and methyl (**12**). The study shows that subtle modifications of the lipophilic periphery of $(RNH)_6P_3N_3$ lead to a variety of supramolecular architectures ranging from 0-D to 2-D

DOI: 10.1039/b212308h

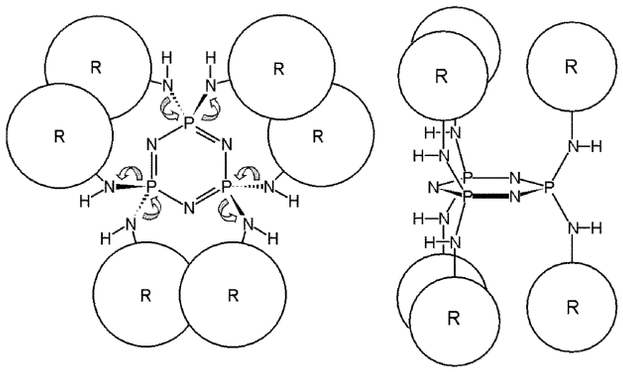

R =

tert-butyl	**1**	phenyl	**7**
cyclohexyl	**2**	*para*-tolyl	**8**
iso-propyl	**3**	*n*-propyl	**9**
benzyl	**4**	allyl	**10**
2-phenylethyl	**5**	propargyl	**11**
iso-butyl	**6**	methyl	**12**

Fig. 1 Schematic representation of the tecton $(RNH)_6P_3N_3$ and the free rotation around P–NH bonds.

structures including monomer, dimer, cyclic hexamer, linear chain, zigzag chain, double chain, graphite type sheet, rectangular grid and hexagonal close-packed sheet.

So far, cyclotriphosphazenes have scarcely been applied in crystal engineering. One example is the use of tris(*o*-phenylenedioxy) cyclotriphosphazene and its derivatives as host-matrices for inclusion compounds.[15] Intermolecular NH ··· N bonds between phosphazene molecules have been observed in the parent compound hexaamino cyclotriphosphazene, $(H_2N)_6P_3N_3$, which forms a supramolecular 3-D network involving all NH and N(ring) sites as H-acceptors and all NH functions as H-donors.[16] Mixed alkoxy-amino derivatives $(RO)_4(H_2N)_2P_3N_3$ also exhibit NH ··· N(ring) and NH ··· NH bonds.[17] The only derivative of $(RNH)_6P_3N_3$ which has been structurally characterised so far is the monomeric adamantyl compound (R = adamantyl). In this case, the steric bulk of the six adamantyl groups prevents intermolecular NH ··· N interactions between phosphazene molecules, allowing only interaction with a $CDCl_3$ molecule in the solid state by forming a CD ··· N(ring) hydrogen bond.[18]

Results

Phosphazene derivatives **1**–**12** were prepared in high yields by reaction of hexachloro cyclotriphosphazene with excess primary amine in the presence of triethylamine in toluene.[19] All products showed single signals in ^{31}P NMR and are chemically and thermally highly stable. This includes unlimited exposure to air, treatment with aqueous acids and bases as well as prolonged heating above melting points. It is also noteworthy that, contrary to previous reports, inert gas protection is not required during synthetic procedures.

With the exception of **5**, **7**, **8** and **12**, phosphazene compounds $(RNH)_6P_3N_3$ crystallise directly from the melt. In some cases this is the only route towards guest-free single crystals. Compound **5** exists as a highly viscous oil at room temperature and solidifies to a glassy material at around 10 °C preventing structural analysis of pure **5**. However, suitable crystals of the solvate **5**·thf were obtained. Crystal structures were determined for **1**, **2**, **3**, **4**, **5**·thf, **6**, **7**, **8**, **9**, **10**, **11** and **12**. Structural parameters of the central P_3N_9 cores are in agreement with literature data for similar species.[20] All the P_3N_3 rings are planar or close to planarity with P–N(ring) bonds (av. 1.60 Å) being shorter than P–NH bonds (av. 1.66 Å).

All derivatives except **1** exhibited intermolecular NH ··· N interactions between phosphazene molecules (Fig. 2). Nine principal types of supramolecular motifs featuring NH ··· N-bridges were observed (Fig. 3) including single (**a**), double (**b**, **c**, **d**) triple (**e**, **f**, **g**, **h**) and quadruple (**j**) H-bridges. The single bridge **a** is formed by the interaction of an NH group of one phosphazene molecule with an N(ring)-atom of another phosphazene molecule. In the bifurcate double bridge **b** the $P(NHR)_2$ unit of one molecule acts as a double H-donor to one N(ring)-atom of a neighbour. In double H-bridges **c** and **d** both molecules simultaneously act as H-donors and H-acceptors *via* NH ··· N(ring) interactions. For **c**, which frequently coincides with a crystallographic inversion centre, NH donors are on opposite faces of neighbouring phosphazene rings which are parallel but displaced vertically forming a shallow step. In arrangement **d** the NH donors are on the same face of both rings, which again are almost parallel, but twisted along the axis of the dimer. The triple bridge **e** features three NH ··· N(ring) interactions and can be regarded as **c** with an extra **b**-type bifurcated bond. The other triply bridged interactions also feature additional NH ··· NH bonds: motif **f** is related to **c**, but has an additional bond, and **g** and **h** correspond to **d** with additional bonds. In contrast to bridge types **a**–**g** the phosphazene rings in the **h**-bridge are oriented nearly orthogonally. Finally, the quadruple H-bridge **j** can be derived from **c**, by adding two additional long NH ··· NH interactions. The N ··· N distances of intermolecular H-bridges are listed in Table 1.

For the majority of structures (except **6**, **8** and **12**), NH-positions were located from difference Fourier maps and refined using similar distance restraints between H and parent N-atoms. A scatterplot, displaying the shortest intermolecular N ··· N distance involving an exocyclic NH moiety (containing freely refined H-atoms) *vs*. the corresponding NH ··· N angles, was used as a diagnostic tool to examine the presence of H-bonding (Fig. 4). Intermolecular NH ··· N bonds exhibiting N ··· N distances below 3.3 Å are close to linearity and can be considered as modestly strong H-bonds. In addition, some weaker NH ··· N contacts are within the range of 3.3 to 3.5 Å. Those weaker contacts accompany stronger NH ··· N bonds within triple and quadruple H-bridges.

The *tert*-butyl derivative **1** crystallises from the melt in space group $P\bar{1}$ and contains two crystallographically independent molecules, which do not undergo intermolecular NH ··· N interactions. The shortest intermolecular N ··· N distance amounts to 4.92 Å. The cyclohexyl compound **2** crystallises from a hot solution of hexane in space group $P\bar{1}$ with one molecule per asymmetric unit. It exists in the solid state as a centrosymmetric dimer linked by a **c**-bridge. The *iso*-propyl derivative **3** crystallises directly from the melt or by evaporation of a hexane solution. Its crystal structure exhibits space group $R\bar{3}$ containing one molecule per crystallographically asymmetric unit. Each molecule interacts with two neighbouring molecules to form a discrete hexameric ring structure of S_6 symmetry, which is held together by six **e**-bridges. The benzyl phosphazene **4** crystallises by slow evaporation of a hexane/thf solution in space group $P2_1$ containing two crystallographically independent molecules. Phosphazenes are connected *via* **c**-bridges to two neighbouring molecules to form zigzag chains. The solvated 2-phenylethyl compound **5**·thf crystallises from a thf/hexane solution in space group $C2/c$ and forms linear chains in the solid-state. Phosphazene molecules are linked by **f**-bridges. Two neighbouring molecules within the chain are symmetrically related *via* *c*-glide planes. In addition, each phosphazene binds one thf molecule, which is accommodated in a cavity formed by four 2-phenylethyl groups. The *iso*-butyl derivative **6** crystallises under anhydrous conditions from the melt in space group $P\bar{1}$ with five molecules in the asymmetric unit forming a chain-type structure. The five independent molecules are connected by an alternating **g**–**j**–**f**–**h**–**g**-bridge pattern. The phenyl derivative **7**

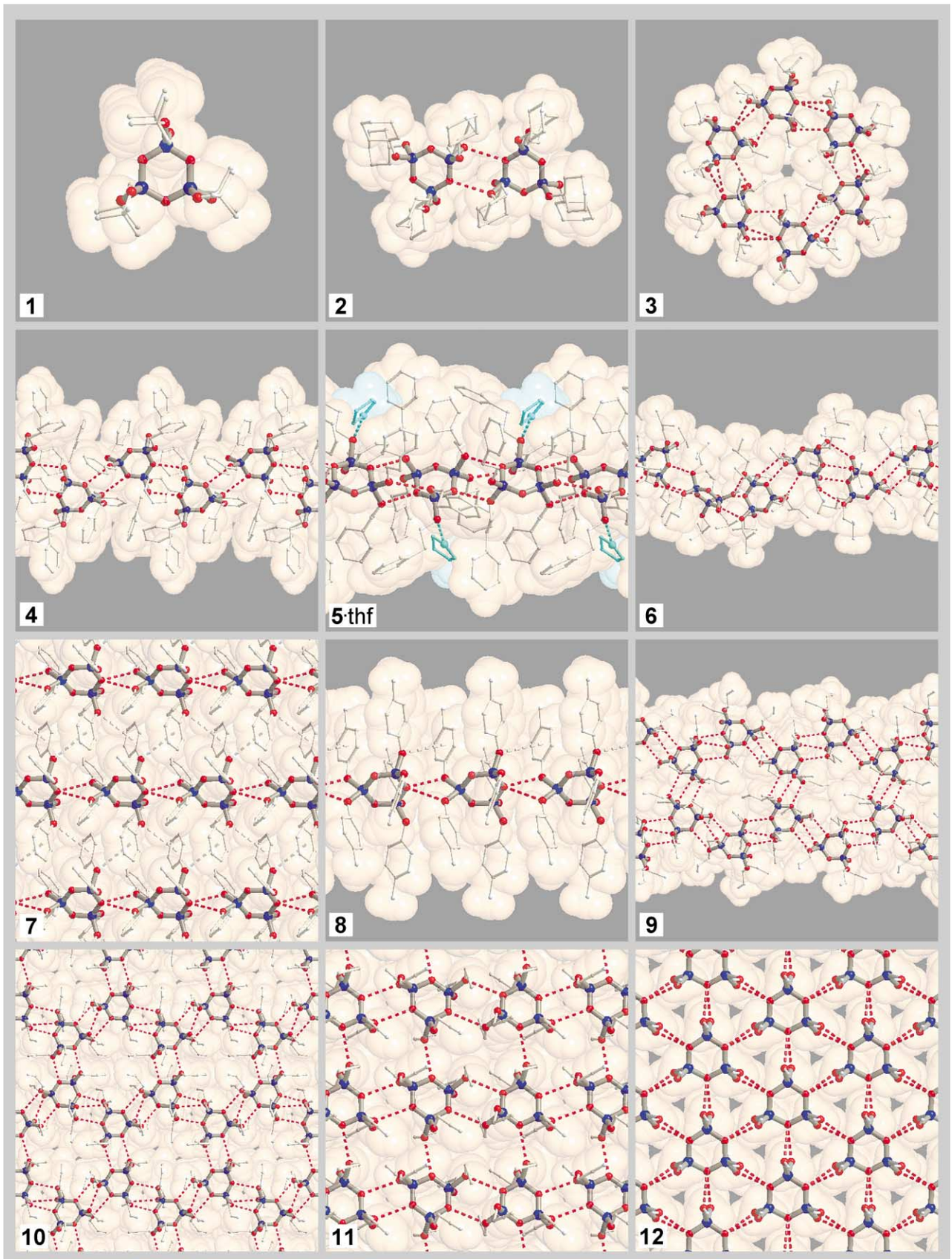

Fig. 2 Crystal structures of **1**, **2**, **3**, **4**, **5**·thf, **6**, **7**, **8**, **9**, **10**, **11** and **12**. Ball-and-stick models are superimposed onto space-filling models, N = red, P = blue, C = grey, thf = turquoise, H-atoms are omitted, NH ··· N interactions are drawn as dashed red lines and NH ··· aryl interactions as dashed grey lines.

crystallises from toluene in space group *C*2, with molecules lined up in a head-to-tail fashion along the two-fold axis connected by symmetrical **b**-bridges. The resulting 1-D chain interacts with neighbouring chains *via* NH ··· aryl interactions (N ··· aryl(centroid) 3.78 Å) to form 2-D sheets in an overall polar arrangement. The *p*-tolyl phosphazene **8** crystallises in space group $P\bar{1}$, with molecules linked by unsymmetrical **b**-bridges showing one short and one long NH ··· N contact to

Table 1 N ··· N distances (Å) of intermolecular H-bridges[a]

Compound	H-bridging motif	N ··· N
2	**c**[b]	3.247(6)
3	**e**	3.155(3), 3.486(4), 3.537(4)
4	**c**	3.071(5), 3.087(5)
	c	3.104(5), 3.194(5)
5·thf	**f**	3.065(2) (r), 3.132(2) (r), 3.321(2) (x)
6	**g**	3.14(2) (r), 3.19(2) (r), 3.18(2) (x)
	j	3.08(2) (r), 3.11(2) (r), 3.57(2) (x), 3.65(2) (x)
	f	3.01(3) (r), 3.34(2) (r), 3.54(3) (x)
	h	3.04(2) (r), 3.10(2) (r), 3.52(2) (x)
	g	3.11(2) (r), 3.50(2) (r), 3.29(2) (x)
7	**b**[c]	3.099(6)
8	**b**	2.942(8), 3.481(8)
9	**g**[d]	3.130(5) (r), 3.235(8) (x)
	g	3.011(5) (r), 3.174(5) (r), 3.213(5) (x)
	g	3.069(5) (r), 3.211(6) (r), 3.230(6) (x)
10	**c**[b]	3.017(5)
	g	2.975(5) (r), 3.158(5) (r), 3.389(5) (x)
	g	3.086(5) (r), 3.433(5) (r), 3.190(5) (x)
11	**a**	2.982(2)
	c[b]	3.099(2)
	c[b]	3.208(2)
12	**b**	3.11(1), 3.13(1)

[a] (r) refers to NH ··· N(ring) and (x) to NH ··· NH interactions. [b] Situated on inversion centre. [c] Situated along two-fold axis. [d] Perpendicular to two-fold axis.

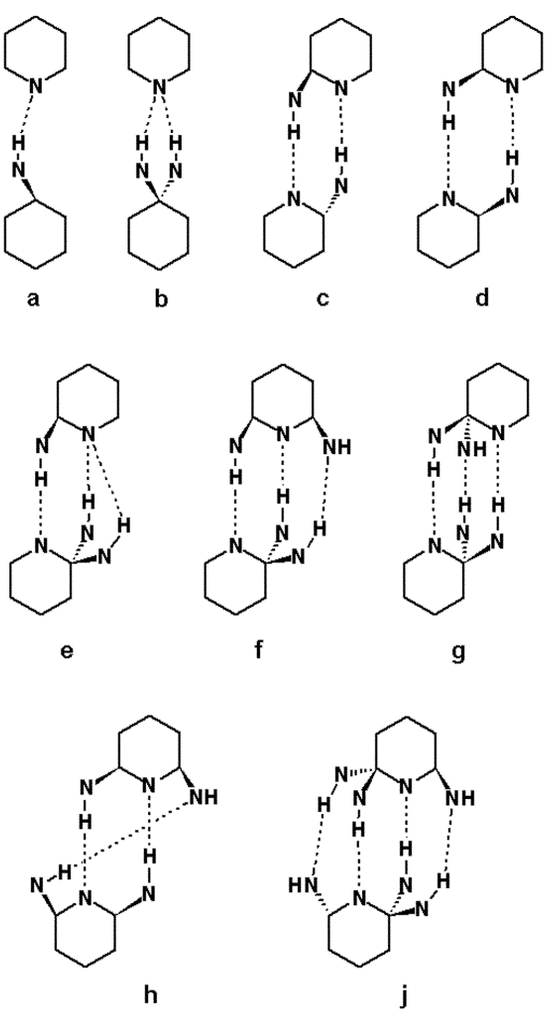

Fig. 3 Schematic representation of H-bridging motifs occurring in solid state structures of $(RNH)_6P_3N_3$ including single (**a**), double (**b**, **c**, **d**), triple (**e**, **f**, **g**, **h**) and quadruple (**j**) H-bridges.

form a linear chain. In addition, intermolecular NH ··· π interactions occur within the chain (N ··· aryl(centroid) 3.74 Å). In contrast to **7**, the crystal structure of **8** forms an

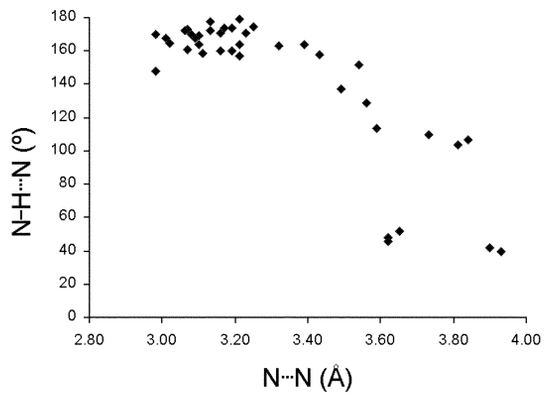

Fig. 4 Scatterplot of the shortest intermolecular N ··· N distances involving exocyclic NH moieties which contain freely refined H-atoms *vs*. the corresponding NH ··· N angles.

overall centrosymmetric arrangement and lacks intermolecular NH ··· π interactions between neighbouring chains, presumably due to the steric bulk of the extra methyl groups. The *n*-propyl compound **9** crystallises directly from the melt in space group *C*2/*c* and forms a double-chain-type arrangement containing two crystallographically independent phosphazene molecules: one interacts with three and the other with two neighbouring molecules. All three crystallographically unique interactions are of the **g**-bridge type. The central **g**-bridge between the two phosphazene molecules connected to three neighbours is located on a crystallographic two-fold axis resulting in the disorder of both bridging and non-bridging hydrogen atoms at the NH ··· NH interaction. The allyl derivative **10** crystallises in space group $P2_1/c$. It forms 2-D graphite-type sheets, in which each phosphazene molecule interacts with three neighbouring molecules. This arrangement contains two crystallographically independent molecules and four unique intermolecular interactions. Two unique **g**-bridges link phosphazenes into zigzag chains, which are then interlinked by two unique **c**-bridges located on inversion centres resulting in an infinite 2-D assembly. The two independent molecules in **10** show different H-acceptor and H-donor behaviour in both **g**-bridges: One molecule acts twice as a double H-donor/single H-acceptor and the other twice as a single H-donor/double H-acceptor. The propargyl phosphazene **11** crystallises from

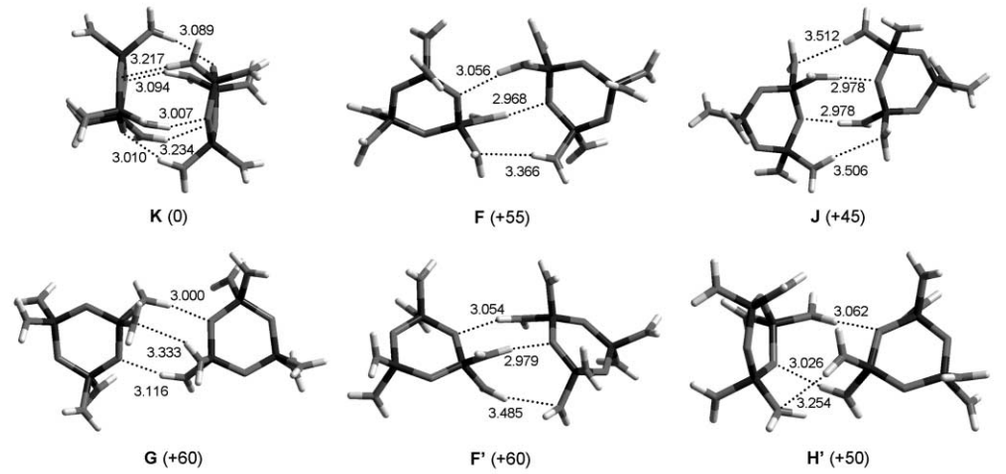

Fig. 5 Optimised structures of gas phase dimers $[(H_2N)_6P_3N_3]_2$ at the HF/3-21G* level of theory. Numbers in brackets refer to potential energies in kJ mol^{-1} relative to **K** (0). Bond parameters refer to N ··· N distances in Å.

thf solution in space group $P2_1/n$ with one molecule per crystallographically asymmetric unit. The overall supramolecular arrangement can be described as a 2-D rectangular grid, in which each molecule interacts with four neighbours. Two neighbours are connected *via* two unique centrosymmetric **c**-bridges in opposite fashion forming linear chains, which are interlinked by **a**-type interactions. The methyl derivative **12** gives plate-like crystals upon evaporation of a methanol solution. Its structure consists of hexagonal close-packed sheets. Each phosphazene molecule interacts with its six neighbours *via* bifurcate **b**-bridges, with all its NH groups acting as H-donors and all its N(ring) sites acting as H-acceptors. The structure displays an alternating arrangement of ordered and disordered layers of phosphazene molecules. Interestingly, the methyl groups also form hexagonal close-packed layers. The centres of the phosphazene rings are located in trigonal prismatic holes between the two hexagonal layers of methyl groups. The number of holes in the hexagonal layer of methyl groups and the number of phosphazene molecules appear in a 3 : 1 ratio. Accordingly, phosphazene molecules of disordered layers are distributed over three positions. The best fit for this structure was obtained in space group *R*3.

In order to understand the multiplicity of H-bonding patterns observed for these phosphazenes, the interaction between two molecules of the unsubstituted compound $(H_2N)_6P_3N_3$ was investigated computationally. Dimers were energy minimised at the HF/3-21G* level, which was found to reproduce well the structure of the monomer.[16] A variety of stable assemblies with three or four H-bridges was found (Fig. 5), all of similar energy relative to the global minimum, a face-to-face complex **K** with six H-bridges. The main types were **G**, which interacts *via* the **g**-bridge, **F**, displaying the **f**-bridge, **F′**, which shows an interaction similar to the **f**-bridge but with a reverse donor–acceptor mode for the NH ··· NH bond, **J**, interacting *via* the quadruple **j**-bridge and **H′**, which features an orthogonal orientation of the two phosphazene rings, similar to the **h**-bridge, but with a slightly different connectivity pattern. Intermolecular N ··· N distances of calculated structures **G**, **F** and **J** compare well with those of crystal structures containing corresponding H-bridge types. Dimers containing the single **a**-bridge or bifurcate bridges **b** and **e** proved to be unstable, at least at this level of theory, and converted into types **G**, **F**, **F′** or **J**.

Discussion

Crystal structures of $(RNH)_6P_3N_3$ show an unprecedented variety of supramolecular aggregation patterns (Fig. 6), considering they are based on one molecular tecton. A range of different intermolecular H-bridging motifs exists and the number of binding partners per molecule varies widely: $(RNH)_6P_3N_3$ can act as monomer (0-connector) **I** (in **1**), undergoing no intermolecular NH ··· N interactions; as a 1-connector binding to one molecule in the dimeric arrangement **II** (in **2**); as a 2-connector resulting in catenation to form either the discrete cyclic hexamer **III** (in **3**), or 1-D assemblies existing as both linear chain **IV** (in **5**, **7**, **8**) or zigzag chains **V** (in **4**, **6**); as a mixed arrangement of 2- and 3-connectors to form the double chain **VI** (in **9**); as a 3-connector to form the graphite type 2-D sheet **VII** (in **10**); as a 4-connector in the rectangular 2-D grid **VIII** (in **11**) and finally as a 6-connector, which occurs in the close-packed hexagonal 2-D sheet **IX** (in **12**).

The degree of aggregation strongly correlates with the steric demand of R, with methyl and *tert*-butyl substituents representing the two opposite ends of the scale. The methyl group in **12** is small enough to allow the most efficient network possible for the phosphazene in two dimensions, whereas the bulkiness of the *tert*-butyl group in monomeric **1**, like the adamantyl group,[18] completely prevents intermolecular NH ··· N bonds. Primary and secondary hydrocarbon substituents form structures of intermediate dimensionality. Alkyl groups branched α to the nitrogen atom give discrete structures, such as dimer **2** and cyclic hexamer **3**. Aryl groups and primary alkyl groups with branching more remote from the phosphazene core form H-bonded 1-D chains. Linear hydrocarbon groups facilitate the formation of supramolecular 2-D networks. The impact of subtle changes within the R-groups on the supramolecular connectivity pattern becomes quite apparent if one looks at systems carrying non-branched C_3 groups: formal dehydrogenation from *n*-propyl C_3H_7 (**9**, 2-/3-connector) to allyl C_3H_5 (**10**, 3-connector) and finally to propargyl C_3H_3 (**11**, 4-connector) leads to higher degrees of networking as the R groups become sterically less demanding.

A key factor influencing the structural variety is the conformational flexibility of the P–NH bond allowing variable directionalities of N–H and N–C_α vectors. However, these are coupled as both are hinged upon the same N-atom, resulting in a strong correlation between the availability of NH sites for intermolecular hydrogen bonding and the size of lipophilic substituents. On one hand, there is the desire to form H-bonds with as many neighbouring molecules as possible. On the other hand, steric effects of R-groups limit the conformational freedom of P–NH bonds, restricting the number of intermolecular contacts. Fig. 7 displays the overall frequency of NH bond directions, which is defined by the absolute torsion angle θ of the X–P–N–H unit, where X represents the centre of the phosphazene ring. It reveals that NH-units acting as H-donors adopt θ-values within a range of 100–140°. Non H-donating NH-units also prefer certain θ-values, which appear in the

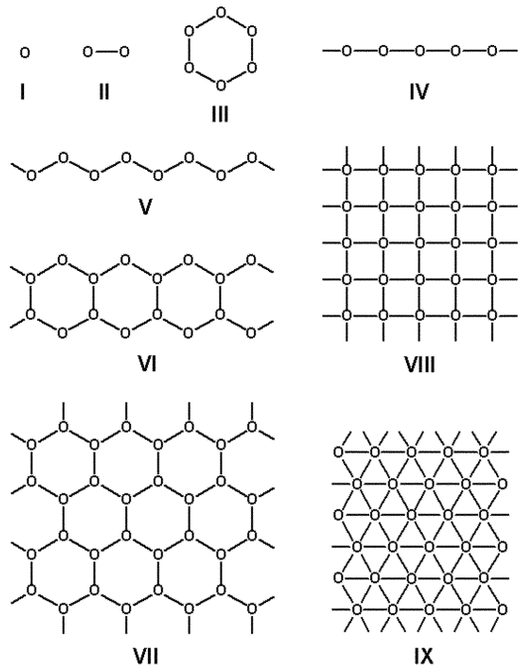

Fig. 6 Schematic representation of aggregation patterns of $(RNH)_6P_3N_3$ in the solid state.

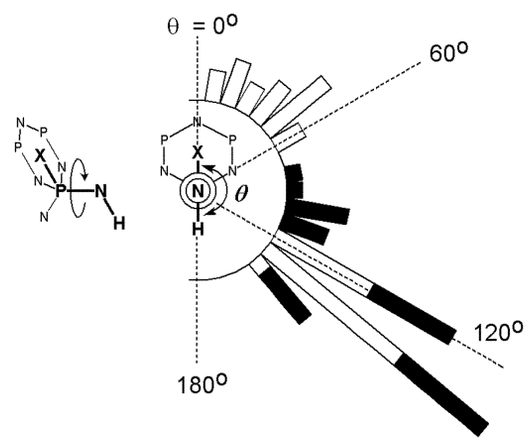

Fig. 7 Frequency of NH bond directions (containing freely refined H-positions) as function of X–P–N–H torsion angles θ, where X is the centroid of phosphazene ring. Black bars indicate involvement of NH units in NH ··· N interactions.

regions 10–70° and 120–140°. The low frequency at $\theta = 0$ and 150–180° can be rationalised by repulsive interactions between geminally arranged NHR units. The gap at $\theta = 70$–120° is presumably a consequence of intramolecular packing effects in order to allow effective interlocking of R-groups on both sides of the phosphazene core.

Although aggregation patterns of $(RNH)_6P_3N_3$ are extremely diverse, some more general observations can be made:

(i) Phosphazene molecules $(RNH)_6P_3N_3$ tend to interact in a 'side-on' fashion rather than 'face-to-face'. The lipophilic hemispheres enclose the assemblies of H-bonded phosphazene cores effectively by forming capsules (around distinct 0-D assemblies), tubular shells (around extended 1-D assemblies) and lipophilic bilayers (around extended 2-D assemblies), respectively. In contrast, M.O. calculations revealed that the face-to-face arrangement **K** is the most stable gas phase dimer of $(H_2N)_6P_3N_3$ presumably because this gives the maximum number of hydrogen bonds in the absence of bulky R groups. Obviously, in the solid-state phosphazenes are not restricted to dimeric assemblies and large numbers of H-bonds can be formed by the build-up of polymeric networks.

(ii) The variety of H-bonding modes **a–h** observed in solid-state structures of $(RNH)_6P_3N_3$ suggests low energy barriers and fast conversion rates from one H-bridge type to another. This assumption is backed up by similar energies of calculated side-on dimer structures **G**, **F**, **F′** and **J**. Concerning possible synthon-conversion mechanisms, there are several possibilities. For example an **e**-bridge can be regarded as an intermediate on the reaction surface between the **c**-bridge and the **d**-bridge. Another example is the reverse donor–acceptor mode of the NH ··· NH bond in calculated gas phase dimers **F** and **F′**, which also occurs in the disordered **g**-bridge of **9**. Transformation from one to the other would only involve reorientation of the two N-bonded protons (NH ··· NH ↔ HN ··· HN). In terms of synthon stability, there appears to be a preference for the **c**- and **g**-bridges. Since the N(exo) atoms are situated about 1 Å off the mean plane of the central phosphazene ring, the phosphazene rings are not in a co-planar arrangement, but are aligned in a parallel terrace-type fashion if linked by the **c**-bridge and are slightly twisted against each other in the **g**-bridge. Both interactions support the 120° supramolecular node, leading to a wide range of aggregates, including the dimer, the cyclic hexamer, the zigzag chain, the double chain and the graphite-type sheet, but also the 180° node as observed in **11**. Although the bifurcate **b**-bridge was not found in gas phase dimers of $(H_2N)_6P_3N_3$, it occurs in the solid state in co-operation with other interactions, such as NH ··· π bonds in **7** and **8** or stabilised within the close-packed arrangement of **12**. The **h**-bridge is a departure from the usually observed co-planar side-on alignment with one phosphazene ring being almost orthogonal to the other. A similar orientation of phosphazenes was observed in the calculated gas phase dimer **H′**. However, the **h**-bridge does not seem to be representative, as it appeared in only one structure (**6**) along with other bridging motifs. Nevertheless, it demonstrates the softness of supramolecular synthons associated with $(RNH)_6P_3N_3$ assemblies. The electrostatic potential maps of phosphazenes **3**, **9** and **12** (Fig. 8) give an indication of the 'slipperiness' of the basic tecton and also illustrate the steric role of the lipophilic R-group. Provided the positive (N-bonded H) and negative (N) regions are not shielded effectively, they can be brought into register to form one of the various H-bridging interactions.

(iii) A large proportion of solid-state structures reported here contain more than one molecule in the crystallographically asymmetric unit including crystal structures of **1**, **4**, **6**, **9** and **10**. This behaviour is often accompanied by the occurrence of the **g**-bridge, which is not compatible with first order symmetry operations, as both binding partners contribute different numbers of H-donor and H-acceptor sites: one molecule acts as single H-donor/double H-acceptor while the other one acts as a double H-donor/single H-acceptor. In contrast, the **c**-bridge, which is the other frequently observed type of interaction, is compatible with inversion symmetry. However, some **c**-bridges lack crystallographic symmetry as observed in the 1-D chain arrangement of **4**. The asymmetric unit of **6** contains five crystallographically independent molecules which are linked by five distinct interactions. This implicates some long-range ordering effects, where, during crystallisation, information is carried forward throughout the entire sequence of five molecules involving 30 unique *iso*-butyl groups.

The N ··· N distances are similar to those found in other systems containing NH ··· N bonds. Although most of H-bridge motifs presented here are unprecedented, there are some resemblances with NH ··· X bridging modes observed in supramolecular assemblies of aromatic heterocycles. The **c**-bridge resembles the centrosymmetric double H-bridge of 2-aminopyridine derivatives[21] and the **b**-bridge is similar to the bifurcate H-bridge found in adducts of urea derivatives.[22] However, in contrast to $(RNH)_6P_3N_3$, where the conformational freedom enables smooth conversion of 3-dimensional

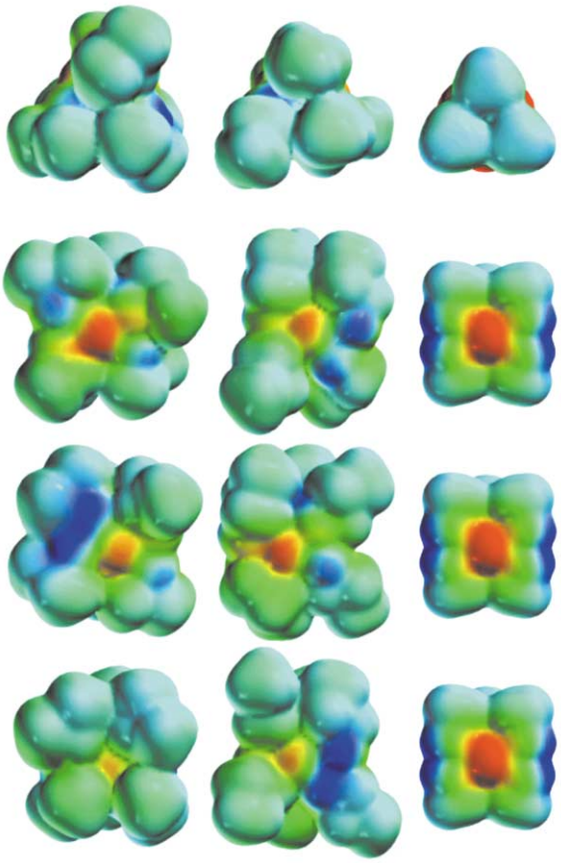

Fig. 8 Electrostatic potential maps calculated on the basis of crystal coordinates of **3** (left column), **9** (middle column) and **12** (right column). Top row: view onto phosphazene rings; bottom rows: side views onto N(ring) sites. Positive regions (N-bonded H) are shown in blue and negative regions (N) in red. Note that, apart from one N(ring) site in **3** (depicted in the bottom left hand corner), all above shown N(ring) sites are involved in H-bridging interactions.

H-bridging motifs, H-bonding between aromatic heterocycles is generally restricted to planar arrangements.

Conclusion

Phosphazenes $(RNH)_6P_3N_3$ display a vast variety of supramolecular structures ranging from the isolated monomer to the hexagonal close-packed sheet. Remarkably, the leap from one aggregation pattern to another is caused by only subtle structural alterations within the lipophilic periphery of the molecule. The parallel equatorial alignment of molecules *via* NH ··· N bonds is a dominant feature of the supramolecular connectivity pattern of $(RNH)_6P_3N_3$, as the R-groups form lipophilic hemispheres effectively encapsulating the H-bonded phosphazene network. H-Bridging modes and packing of lipophilic R-groups are strongly correlated *via* rotation around the P–NH bond. The exceptional synthon-softness, which is displayed by the wide range of H-bridging motifs, and the tendency to form highly ordered materials in a rather effortless manner suggests a smooth, thermodynamically controlled assembly process, in which the conformational flexibility of the molecule plays a central role. Many biomolecules show a similarly flexible assembly behaviour based on soft synthons and soft tectons. For example, the complex but highly selective build-up of secondary and tertiary structures of proteins depends on the interplay of side chain packing and hydrogen bonding.[23] The highly inert and straightforwardly synthesised phosphazenes $(RNH)_6P_3N_3$, in conjunction with the smooth crystallisation process, provide an interesting platform for the arrangement of multifunctional arrays, which might find applications as ultra-soft tectons not only in crystal engineering, but also other areas such as mesophase materials and molecular receptor systems.

Experimental

General procedures

FT-IR spectra were recorded on a Perkin-Elmer Paragon 1000 spectrometer in Nujol between CsI plates. NMR spectra were recorded at 25 °C on a Bruker AMX 400 spectrometer [^{1}H NMR (400.13 MHz, TMS), ^{13}C{^{1}H} NMR (100.62 MHz, TMS), ^{31}P{^{1}H} NMR (161.97 MHz, 85% H_3PO_4(ext.)]. Hexachloro cyclotriphosphazene (Aldrich) was used as received. Solvents were freshly distilled from alkali metals (toluene from sodium; thf and hexane from potassium). Amines were distilled from KOH and stored over molecular sieves.

Synthesis of 1–12

To a stirred solution of 10 g (28.8 mmol) hexachloro cyclotriphosphazene in 200 ml toluene and 100 ml triethylamine was added 345 mmol of primary amine at room temperature. The formation of a white precipitate indicated the onset of the reaction. The solution was heated to reflux until substitution was completed (^{31}P NMR control) and cooled prior to filtration (in the case of **1** the reaction was carried out in an autoclave at 130 °C). The solvent and excess amines were removed under reduced pressure yielding the hexakis(organoamino) cyclotriphosphazene. Phosphazenes **3**, **6**, **7**, **9** and **12** were obtained as hydrochloride adducts. Hydrochloride adducts **3**·HCl, **6**·HCl, **9**·HCl and **12**·HCl were stirred with finely ground potassium hydroxide in diethyl ether for 12 hours. The solvent was removed *in vacuo* and the residue extracted with toluene. The hydrochloride **7**·HCl was treated with aqueous KOH and extracted with diethyl ether.

Hexakis(*tert*-butylamino)cyclotriphosphazene (1). Colourless crystals were obtained by slow cooling of the melt under an inert gas atmosphere (yield 75%). Mp: 164 °C. $C_{24}H_{60}N_9P_3$ (567.72) calc. C, 50.77; H, 10.65; N, 22.20. Found C, 50.90; H, 10.82; N, 21.98%. ^{1}H NMR ($CDCl_3$): δ 1.29 (s, 54H, CH_3), 2.09 (s, 6H, NH). ^{13}C{^{1}H} NMR ($CDCl_3$): δ 31.3 (CH_3), 51.5 (NC). ^{31}P{^{1}H} NMR (toluene) δ 8.5. IR ν/cm^{-1}: 3412 (ν_s N–H), 3386 (ν_s N–H), 1363, 1243, 1225, 1209, 1166 (ν_s P–N_{ring}), 1018, 922, 895, 851, 807, 743.

Hexakis(cyclohexylamino)cyclotriphosphazene (2). Colourless crystals were obtained from a hot hexane solution (yield 84%). Mp: 159 °C. $C_{42}H_{72}N_9P_3$ (723.85): calc. C, 59.72; H, 10.02; N, 17.41. Found C, 59.58; H, 10.05; N, 17.32%. ^{1}H NMR ($CDCl_3$): δ 0.86–1.67 (m, 60H, CH_2), 2.16 (m, 6H, CH), 3.34 (s, 6H, NH). ^{13}C{^{1}H} NMR ($CDCl_3$): δ 25.8 (CH_2), 26.3 (CH_2), 36.8 (CH_2), 50.1 (CH). ^{31}P{^{1}H} NMR (toluene): δ 14.9. IR ν/cm^{-1}: 3406 (ν_s N–H), 3336 (ν_s N–H), 3263 (ν_s N–H), 1445, 1409, 1287, 1262, 1233, 1198 (ν_s P–N_{ring}), 1143, 1109, 1095, 1050, 1020, 994, 905, 885, 846, 819, 802, 774.

Hexakis(*iso*-propylamino)cyclotriphosphazene (3). Colourless crystals were obtained from slow evaporation of a hexane solution (yield 88%). Mp: 83 °C. $C_{18}H_{48}N_9P_3$ (483.56): calc. C, 44.71; H, 10.00; N, 26.07. Found C, 44.63; H, 10.05; N, 25.91%. ^{1}H NMR ($CDCl_3$): δ 1.06 (s, 36H, CH_3), 1.81 (s, 6H, CH), 3.35 (s, 6H, NH). ^{13}C{^{1}H} NMR ($CDCl_3$): δ 24.3 (CH_3), 41.6 (CH). ^{13}P{^{1}H} NMR (toluene): δ 14.7. IR ν/cm^{-1}: 3411 (ν_s N–H), 3224 (ν_s N–H), 1398, 1362, 1297, 1260, 1207, 1156 (ν_s P–N_{ring}), 1016, 888, 856, 795, 752.

Hexakis(benzylamino)cyclotriphosphazene (4). Colourless crystals were obtained from slow evaporation of a thf/hexane solution (yield 79%). Mp: 82 °C. $C_{42}H_{48}N_9P_3$ (771.82): calc. C, 65.36; N, 16.33; H, 6.27. Found C, 65.13; N, 16.35; H, 6.25%.

^{1}H NMR ($CDCl_3$): δ 2.66 (br, 6H, NH) 4.13, 4.15 (d, 12H, CH_2, $^3J_{H–H}$ = 3.9 Hz), 6.99–7.32 (m, 30H, Ph). $^{13}C\{^1H\}$ NMR ($CDCl_3$): δ 45.7 (CH_2), 127.2 (Ph), 128.1 (Ph), 128.9 (Ph). $^{13}P\{^1H\}$ NMR (toluene): δ 19.8. IR ν/cm^{-1}: 3377 (ν_s N–H), 3167 (ν_s N–H), 1603 (ν_s C–C_{aryl}),1494, 1301,1182 (ν_s P–N_{ring}), 1097, 1028, 927, 902, 851, 780, 777, 695.

Hexakis(2-phenylethylamino)cyclotriphosphazene (5). Colourless crystals of **5**·thf were obtained from a thf/hexane solution stored at −20 °C (yield 71%). Mp: 10 °C. $C_{48}H_{60}N_9P_3$ (855.95): calc. C, 67.34; N, 14.76; H, 7.06. Found C, 66.95; N, 14.47; H, 7.29%. ^{1}H NMR ($CDCl_3$): δ 2.25 (m, 6H, NH), 2.68 (m, 12H, NHCH_2), 3.08 (t, 12H, NHCH_2CH_2), 7.15 (m, 36H, Ph). $^{13}C\{^1H\}$ NMR ($CDCl_3$): δ 38.0 (CH_2), 42.2 (CH_2), 126.3 (*o*-C), 128.5 (*p*-C), 128.7 (*m*-C), 139.3 (N–C). $^{13}P\{^1H\}$ NMR (toluene): δ 18.3. IR ν/cm^{-1}: 3390 (ν_s N–H), 3236 (ν_s N–H), 3025 (ν_s N–H), 1602 (ν_s C–C_{aryl}), 1185 (ν_s P–N_{ring}), 1087, 1029, 906, 748, 697.

Hexakis(*iso*-butylamino)cyclotriphosphazene (6). Colourless crystals were obtained by slow cooling from the melt under an inert gas atmosphere (yield 86%). Mp: 67 °C. $C_{24}H_{60}N_9P_3$ (567.71): calc. C, 50.77; H, 10.65; N, 22.21. Found C, 50.17; H, 10.80; N, 21.97%. ^{1}H NMR ($CDCl_3$): δ 0.89 (d, 36H, CH_3, $^3J_{H–H}$ = 6.8 Hz), 1.69 (m, 6H, CH), 2.11 (br, 6H, NH), 2.71 (m, 12H, CH_2). $^{13}C\{^1H\}$ NMR ($CDCl_3$): δ 20.6 (CH_3), 30.3 (CH), 49.2 (CH_2). $^{13}P\{^1H\}$ NMR (toluene): δ 18.68. IR ν/cm^{-1}: 3311 (ν_s N–H), 3175 (ν_s N–H), 1401, 1252, 1188 (ν_s P–N_{ring}), 1138, 1089, 921,817, 776.

Hexakis(anilino)cyclotriphosphazene (7). Colourless crystals were obtained from a toluene solution (yield 78%). Mp: 270 °C. $C_{36}H_{36}N_9P_3$ (687.65): calc. C, 62.88; N, 18.33; H, 5.27. Found C, 62.36; N, 17.95; H, 5.42%. ^{1}H NMR (d_8-thf): δ 6.33 (m, 1H, NH), 6.56, (t, *p*-H, $^3J_{H–H}$ = 7.4 Hz), 6.87 (t, 2H, *m*-H, $^3J_{H–H}$ = 7.4 Hz), 7.02 (d, 2H, *o*-H, $^3J_{H–H}$ = 7.4 Hz). $^{13}C\{^1H\}$ NMR (d_8-thf): δ 117.6 (*o*-*C*), 119.1 (*p*-*C*), 127.8 (*m*-*C*), 142.2 (NC). $^{13}P\{^1H\}$ NMR (thf): δ 3.21. IR ν/cm^{-1}: 3357 (ν_s N–H), 1601 (ν_s C–C_{aryl}), 1287, 1235, 1188 (ν_s P–N_{ring}), 1173 (ν_s P–N_{ring}), 1077, 1027, 936, 862, 748, 693.

Hexakis(*para*-tolylamino)cyclotriphosphazene (8). Colourless crystals were formed from a hexane/thf solution (yield 70%). Mp: 190 °C. $C_{42}H_{48}N_9P_3$ (771.32): calc. C, 65.46; N, 16.31; H, 6.28. Found C, 65.73; N, 15.98; H, 6.81%. ^{1}H NMR (d_8-thf): δ 2.11 (s, 3H, CH_3), 5.31 (m, 1H, NH), 6.86 (s, 4H, Ph). $^{13}C\{^1H\}$ NMR (d_8-thf): δ 20.6 (CH_3), 119.6 (*o*-CH), 129.4 (*m*-CH), 131.2 (*C*CH_3), 137.5 (NC). $^{13}P\{^1H\}$ NMR (thf): δ 2.4. IR ν/cm^{-1}: 3381 (ν_s N–H), 3186 (ν_s N–H), 1613 (ν_s C–C_{aryl}), 1514, 1286, 1174 (ν_s P–N_{ring}), 941, 812.

Hexakis(*n*-propylamino)cyclotriphosphazene (9). Colourless crystals were obtained from a hexane solution stored at 5 °C (yield 85%). Mp: 68 °C. $C_{18}H_{48}N_9P_3$ (483.57): calc. C, 44.71; H, 10.00; N, 26.08. Found C, 44.31; H, 10.15; N, 25.83%. ^{1}H NMR ($CDCl_3$): δ 0.82 (t, 18H, CH_3, $^3J_{H–H}$ = 7.3 Hz), 1.42 (m, 12H, CH_2), 2.00 (br, 6H, NH), 2.79 (m, 12H, NCH_2). $^{13}C\{^1H\}$ NMR ($CDCl_3$): δ 10. 5 (CH_3), 24.2 (CH_2), 41.9 (NCH_2). $^{13}P\{^1H\}$ NMR (toluene): δ 18.6. IR ν/cm^{-1}: 3509 (ν_s N–H), 3300 (ν_s N–H), 1170 (ν_s P–N_{ring}), 1108, 1030, 1004, 890, 853, 790, 733.

Hexakis(allylamino)cyclotriphosphazene (10). Pale yellow crystals were obtained by slow evaporation of a methanol solution (yield 95%). Mp: 87 °C. $C_{18}H_{36}N_9P_3$ (471.51): calc. C, 45.85; H, 7.70; N, 26.74. Found C, 45.69; H, 7.73; N, 26.77%. ^{1}H NMR ($CDCl_3$): δ 2.30 (br, 6H, NH), 3.56 (m, 12H, NCH_2), 5.12 (dd, 12H, CH=CH_2, $^2J_{H–H(gem)}$ = 1.7 Hz, $^3J_{H–H(trans)}$ = 17.1 Hz, $^3J_{H–H(cis)}$ = 10.2 Hz), 5.92 (m, 6H, C*H*=CH_2). $^{13}C\{^1H\}$ NMR ($CDCl_3$): δ 43.6 (NCH_2), 114.5 (CH=*C*H_2), 137.5 (*C*H=CH_2). $^{13}P\{^1H\}$ NMR (toluene): δ 18.9. IR ν/cm^{-1}: 3185 (ν_s N–H), 1641 (ν_s C=C), 1415, 1175 (ν_s P–N_{ring}), 1130 (ν_s P–N_{ring}), 1091, 1027, 998, 910, 856, 792, 723, 557.

Hexakis(propargylamino)cyclotriphosphazene (11). Yellow crystals were obtained by slow evaporation of a methanol solution (yield 90%). Mp: 116 °C. $C_{18}H_{24}N_9P_3$ (459.37): calc. C, 47.06; H, 5.27; N, 27.45. Found C, 46.62; H, 5.33; N, 27.50%. ^{1}H NMR ($CDCl_3$): δ 1.66 (br, 6H, NH), 2.65 (br, 6H, CH), 3.69 (br, 12H, CH_2). $^{13}C\{^1H\}$ NMR ($CDCl_3$): δ 29.5 (CH_2), 69.7 (CH), 81.9 (CH). $^{13}P\{^1H\}$ NMR (toluene): δ 17.8. IR ν/cm^{-1}: 3407, 3371, 3289 (ν_s N–H), 3197 (ν_s N–H), 1409, 1350, 1244, 1226, 1180 (ν_s P–N_{ring}), 1103, 979, 901, 842, 782, 673, 650, 631.

Hexakis(methylamino)cyclotriphosphazene (12). Colourless crystals were obtained by slow evaporation of a methanol solution (yield 37%). Mp: 258 °C. $C_6H_{24}N_9P_3$ (315.27): calc. C, 22.86; H, 7.67; N, 39.99. Found C, 22.58; H, 7.80; N, 39.80%. ^{1}H NMR ($CDCl_3$): δ 2.02 (s, 6H, NH), 2.46 (s, 18H, CH_3). $^{13}C\{^1H\}$ NMR ($CDCl_3$): δ 26.1. $^{13}P\{^1H\}$ NMR (toluene): δ 22.7. IR ν/cm^{-1}: 3311 (ν_s N–H), 3183 (ν_s N–H), 1259, 1184 (ν_s P–N_{ring}), 1136, 1099, 825, 688.

Crystallography

Crystal data were collected on Bruker-AXS Smart Apex CCD (**1**, **3**, **4**, **5**·thf, **6**, **8**, **9**, **10**, **11**), Stoe IPDS (**7**, **12**) and Rigaku AFC6S (**2**) diffractometers using graphite monochromated Mo-Kα radiation (λ = 0.71073 Å). Structures were solved by direct methods and structures refined by full-matrix least-squares based on all data using F^2.[24] Crystal data are listed in Table 2. Non-H atoms were refined anisotropically, unless otherwise stated. H-atoms were placed in calculated positions, except positions of N-bonded H atoms in **1**, **2**, **3**, **4**, **5**·thf, **7**, **9**, **10** and **11**, which were refined freely using similar distance restraints for all N–H bonds. H-atoms were treated isotropically using the 1.2 fold U_{iso} value of the parent atom except methyl protons, which were assigned the 1.5 fold U_{iso} value of the parent C-atom.

3: Two *iso*-propyl groups are disordered. Disordered atomic positions were split and refined isotropically using similar distance and similar *U* restraints and one occupancy parameter per disordered group.

4: One $P(NHCH_2Ph)_2$ moiety and one benzyl group of one of the two crystallographically unique molecules and one benzyl group of the other molecule are disordered. Disordered atomic positions were split and refined isotropically using similar distance and similar *U* restraints and one occupancy parameter per disordered group.

5·thf: The thf molecule is disordered. Disordered atomic positions were split and refined using similar distance and similar *U* restraints and one occupancy parameter for the disordered group.

6: Crystals were of high mosaicity and gave a weak diffraction pattern of low resolution. Therefore, the reflection set was cut off at $2\theta = 40°$. N and C positions were refined isotropically. One *iso*-butyl group is disordered. Disordered atomic positions were split using similar distance and similar *U* restraints and one occupancy parameter for the disordered group.

8: Crystals were of high mosaicity, which did not allow the free refinement of N-bonded H-atoms.

9: Nine *n*-propyl groups are disordered. Disordered atomic positions were split and refined using similar distance and similar *U* restraints and one occupancy parameter per disordered group.

10: Crystals are non-merohedrally twinned. There is some overlap of reflections between domains, which hampers the determination of intensities and leads to the high *R*-value. Three allyl groups are disordered. Disordered atomic positions were split and refined isotropically using similar distance and similar *U* restraints and one occupancy parameter per disordered group.

Table 2 Crystal data for **1**–**12**

	1	**2**	**3**	**4**	**5**·thf	**6**	**7**	**8**	**9**	**10**	**11**	**12**
Chemical formula	$C_{24}H_{60}N_9P_3$	$C_{36}H_{72}N_9P_3$	$C_{18}H_{48}N_9P_3$	$C_{42}H_{48}N_9P_3$	$C_{52}H_{68}N_9OP_3$	$C_{24}H_{60}N_9P_3$	$C_{36}H_{36}N_9P_3$	$C_{42}H_{48}N_9P_3$	$C_{18}H_{48}N_9P_3$	$C_{18}H_{36}N_9P_3$	$C_{18}H_{24}N_9P_3$	$C_6H_{24}N_9P_3$
Formula weight	567.72	723.94	483.56	771.80	928.06	567.72	687.65	771.80	483.56	471.47	459.37	315.25
Crystal system	Triclinic	Triclinic	Rhombohedral	Monoclinic	Monoclinic	Triclinic	Monoclinic	Triclinic	Monoclinic	Monoclinic	Monoclinic	Rhombohedral
Space group	$P\bar{1}$	$P\bar{1}$	$R\bar{3}$	$P2_1$	$C2/c$	$P\bar{1}$	$C2$	$P\bar{1}$	$C2/c$	$P2_1/c$	$P2_1/n$	$R3$
a/Å	10.424(2)	11.039(4)	36.840(10)	11.627(3)	33.828(3)	13.424(7)	18.160(4)	7.224(4)	42.210(5)	11.552(6)	13.352(2)	7.0898(10)
b/Å	11.404(2)	12.001(4)	36.840(10)	24.689(3)	12.5140(10)	14.344(8)	7.1790(10)	10.017(6)	11.3419(12)	20.301(13)	7.3886(9)	7.0898(10)
c/Å	14.704(2)	16.651(6)	10.799(4)	15.391(2)	25.588(2)	24.639(13)	13.001(3)	28.331(15)	23.092(3)	21.372(11)	22.943(3)	51.178(10)
α/°	101.117(3)	95.81(4)	90	90	90	89.324(10)	90	90.054(11)	90	90	90	90
β/°	108.382(3)	91.38(4)	90	111.950(10)	111.073(10)	87.424(11)	95.22(3)	91.593(11)	91.105(2)	94.17(3)	101.712(3)	90
γ/°	90.023(3)	108.77(3)	120	90	90	65.306(9)	90	107.718(7)	90	90	90	120
V/Å^3	1624.1(5)	2074.1(13)	12693(7)	4097.9(13)	10107.5(14)	4306(4)	1687.9(6)	1952(2)	11053(2)	4999(5)	2216.2(5)	2227.8(6)
T/K	150	200	150	150	150	150	200	150	150	150	150	200
Z	2	2	18	4	8	5	2	2	16	8	4	6
μ(Mo-Kα)/cm^{-1}	0.212	0.180	0.233	0.187	0.165	0.200	0.218	0.197	0.238	0.262	0.294	0.401
ρ(calc)/gcm^{-1}	1.161	1.159	1.139	1.251	1.220	1.095	1.353	1.313	1.162	1.253	1.377	1.410
Reflections, total	9422	5717	19266	16189	20873	13197	3788	7889	28263	25137	13224	4515
Reflections, unique	7736	5408	4045	8648	8915	10124	2563	5004	9739	25137	5119	1527
$R1$ ($F > 4\sigma(F)$)	0.0462	0.0611	0.0492	0.0372	0.0425	0.0927	0.0337	0.0793	0.0621	0.0904	0.0360	0.0989
$wR2$ (all data)	0.1038	0.1451	0.1320	0.0824	0.1147	0.2310	0.0700	0.2158	0.2038	0.2399	0.0867	0.2657
Flack parameter	0.47(8)			0.65(9)		0.2(2)	−0.02(13)					0.7(5)

12: There is an alternation of ordered and disordered H-bonded phosphazene sheets. Refinement in space group $R3$ gives the best agreement factors. Other possibilities were also tested, including $R\bar{3}$, $R32$, $R3m$ and merohedral twinning in both rhombohedral and monoclinic C settings. The phosphazene molecule of the disordered sheet is disordered over three positions and was refined isotropically using similar distance and similar U restraints. An occupation factor of 1/3 was used for all atomic positions of the disordered sheet.

CCDC reference numbers 199621–199632.

See http://www.rsc.org/suppdata/dt/b2/b212308h/ for crystallographic data in CIF or other electronic format.

M.O. Calculations

Energy minimizations and electrostatic potential maps were calculated using Spartan (Wavefunction Inc.). At the HF/3-21G* level $(NH_2)_6P_3N_3$ has a planar P_3N_3 core with P–N(ring) bond lengths of 1.587 Å, P–NH_2 bond lengths of 1.647 Å, and N–P–N bond angles of 104°. This is comparable to the crystal structure of $(NH_2)_6P_3N_3$[16] which has a planar P_3N_3 core with P–N(ring) bond lengths of 1.60 (±0.01) Å, P–NH_2 bond lengths of 1.65 (±0.01) Å, and N–P–N bond angles of 103 (±2)°. Dimers of $(NH_2)_6P_3N_3$ were energy minimized from a large number of starting geometries, including the **a**, **b** and **e** motifs, and generally converged to one of the arrangements shown in Fig. 5, or mirror image versions of these. No corrections were made for basis set superposition errors.

Acknowledgements

This work was supported by the EPSRC (GR/N36851) and the Royal Society.

References

1 (*a*) J. M. Lehn, *Supramolecular Chemistry: Concepts and Perspectives*, VCH, Weinheim, 1995; (*b*) T. Steiner, *Angew. Chem., Int. Ed.*, 2002, **41**, 48; (*c*) J. Bernstein, M. C. Etter and L. Leiserowitz, in *Structure Correlation*, vol. 2, eds. H.-B. Bürgi and J. D. Dunitz, VCH, Weinheim, 1994, p. 431.

2 (*a*) G. R. Desiraju, *Angew. Chem., Int. Ed. Engl.*, 1995, **34**, 2311; (*b*) S. Subramanian and M. J. Zaworotko, *Coord. Chem. Rev.*, 1994, **137**, 357; (*c*) J. C. MacDonald and G. M. Whitesides, *Chem. Rev.*, 1994, **94**, 2383; (*d*) B. Moulton and M. J. Zaworotko, *Chem. Rev.*, 2001, **101**, 1629; (*e*) M. J. Zaworotko, *Chem. Commun.*, 2001, 1; (*f*) L. R. McGillivray and J. L. Atwood, *Angew. Chem., Int. Ed.*, 1999, **38**, 1019; (*g*) L. J. Prins, D. N. Reinhoudt and P. Timmerman, *Angew. Chem., Int. Ed.*, 2001, **40**, 2382.

3 (*a*) X. Wang, M. Simard and J. D. Wuest, *J. Am. Chem. Soc.*, 1994, **116**, 12119; (*b*) D. Su, X. Wang, M. Simard and J. D. Wuest, *Supramol. Chem.*, 1995, **6**, 171.

4 M. Bailey and C. J. Brown, *Acta Crystallogr.*, 1967, **22**, 387.

5 (*a*) D. J. Duchamp and R. E. Marsh, *Acta Crystallogr., Sect. B*, 1969, **25**, 5; (*b*) F. H. Herbstein, *Top. Curr. Chem.*, 1987, **140**, 107; (*c*) S. V. Kolotuchin, P. A. Thiessen, E. F. Fenlon, S. R. Wilson, C. J. Loweth and S. C. Zimmermann, *Chem. Eur. J.*, 1999, **5**, 2537.

6 O. Ermer, *J. Am. Chem. Soc.*, 1988, **110**, 3747.

7 (*a*) R. Alcala and S. Martinez, *Acta Crystallogr., Sect. B*, 1972, **28**, 1671; (*b*) J. Yang, J. L. Marendaz, S. J. Geib and A. D. Hamilton, *Tetrahedron Lett.*, 1994, **35**, 3665; (*c*) S. Valiyaveettil and K. Müllen, *New J. Chem.*, 1998, **22**, 89.

8 (*a*) J. A. Zerowski, C. T. Seto, D. A. Wierda and G. M. Whitesides, *J. Am. Chem. Soc.*, 1990, **112**, 9025; (*b*) J. A. Zerowski, C. T. Seto and G. M. Whitesides, *J. Am. Chem. Soc.*, 1992, **114**, 5473.

9 (*a*) N. H. Buttrus, R. I. Damja, C. Eaborn, P. B. Hitchcock and P. D. Lickiss, *J. Chem. Soc., Chem. Commun.*, 1985, 1385; (*b*) S. S. Al-Juaid, N. H. Buttrus, R. I. Damja, Y. Derouchi, C. Eaborn, P. B. Hitchcock and P. D. Lickiss, *J. Organomet. Chem.*, 1989, **371**, 287.

10 (*a*) P. Jutzi, M. Schneider, H.-G. Stammler and B. Neumann, *Organometallics*, 1997, **16**, 5377; (*b*) R. Murugavel, V. Chandrasekhar, A. Voigt, H. W. Roesky, H.-G. Schmidt and M. Noltemeyer, *Organometallics*, 1995, **14**, 5298.

11 (*a*) N. Winkhofer, H. W. Roesky, M. Noltemeyer and W. T. Robinson, *Angew. Chem., Int. Ed. Engl.*, 1992, **31**, 599; (*b*) P. Jutzi,

G. Strassburger, M. Schneider, H.-G. Stammler and B. Neumann, *Organometallics*, 1996, **15**, 2842.
12 H. Ishida, J. L. Koenig and K. C. Gardner, *J. Chem. Phys.*, 1982, **77**, 5748.
13 (*a*) R. A. Shaw, B. W. Fitzsimmons and B. C. Smith, *Chem. Rev.*, 1962, **62**, 247; (*b*) H. R. Allcock, *Chem. Rev.*, 1972, **72**, 315.
14 (*a*) A. Steiner, S. Zacchini and P. I. Richards, *Coord. Chem. Rev.*, 2002, **227**, 193; (*b*) A. Steiner and D. S. Wright, *Angew. Chem., Int. Ed. Engl.*, 1996, **35**, 636; (*c*) G. T. Lawson, F. Rivals, M. Tascher, C. Jacob, J. F. Bickley and A. Steiner, *Chem. Commun.*, 2000, 341; (*d*) G. T. Lawson, C. Jacob and A. Steiner, *Eur. J. Inorg. Chem.*, 1999, 1881.
15 (*a*) H. R. Allcock, *J. Am. Chem. Soc.*, 1964, **86**, 5140; (*b*) H. R. Allcock, A. P. Primrose, N. J. Sunderland, A. L. Rheingold, I. A. Guzei and M. Parvez, *Chem. Mater.*, 1999, **11**, 1243; (*c*) T. Kobayashi, S. Isoda and K. Kubono, in *Comprehensive Supramolecular Chemistry*, vol. 6, eds. J. L. Atwood, J. E. D. Davies, D. D. Macnicol and F. Vögtle, Elsevier, Pergamon, 1996.
16 F. Golinski and H. Z. Jacobs, *Z. Anorg. Allg. Chem.*, 1994, **620**, 965.
17 J. K. Fincham, H. G. Parks, L. S. Shaw, R. A. Shaw and M. B. Hursthouse, *J. Chem. Soc., Dalton Trans.*, 1988, 1169.
18 W. E. Krause, M. Parvez, K. B. Visscher and H. R. Allcock, *Inorg. Chem.*, 1996, **35**, 6337.
19 See also: (*a*) C. W. Allen, *Chem. Rev*, 1991, **91**, 119; (*b*) S. K. Ray and R. A. Shaw, *J. Chem Soc.*, 1961, 872; (*c*) V. Chandrasekhar, K. Vivekanandan, S. Nagendran, G. T. Senthil Andavan, N. R. Weathers, J. C. Yarbrough and A. W. Cordes, *Inorg. Chem.*, 1998, **37**, 6192.
20 J. R. Rettig and J. Trotter, *Can. J. Chem.*, 1973, **51**, 1295.
21 (*a*) M. Chao, E. Schempp and R. D. Rosenstein, *Acta Crystallogr., Sect. B*, 1975, **31**, 2922; (*b*) J. E. Johnson and R. A. Jacobson, *Acta Crystallogr., Sect. B*, 1973, **29**, 1973; (*c*) G. J. Pyrka and A. A. Pinderton, *Acta Crystallogr., Sect. C*, 1992, **48**, 91; (*d*) H. Schödel, C. Näther, H. Bock and F. Butenschön, *Acta Crystallogr., Sect. B*, 1996, **52**, 842; (*e*) M. Polamo, T. Repo and M. Leskela, *Acta Chem. Scand.*, 1997, **51**, 325.
22 (*a*) C. E. Etter, Z. Urbanczyk-Lipowska, M. Zia-Ebrahimi and T. W. Panunto, *J. Am. Chem. Soc.*, 1990, **112**, 8415; (*b*) R. Thaimattam, D. S. Reddy, F. Xue, T. C. W. Mak, A. Nangia and G. R. Desijaru, *J. Chem. Soc., Perkin Trans. 2*, 1998, 1783; (*c*) P. Le Magueres, L. Ouahab, A. Hocquet and J. Fournier, *Acta Crystallogr., Sect. C*, 1994, **50**, 1507.
23 (*a*) See for example: A. Fersht, *Structure and Mechanism in Protein Science*, 3rd edn., Freeman, New York, 1999; (*b*) K. P. Murphy, *Protein Structure, Stability and Folding*, Humana Press, Totowa, NJ, 2001.
24 G. M. Sheldrick, SHELX97, Program for crystal structure determination, Universität Göttingen, 1997.